

Planetary interiors: Magnetic fields, Convection and Dynamo Theory

2. Convection in planetary interiors

Chris Jones, Department of Applied Mathematics
University of Leeds UK

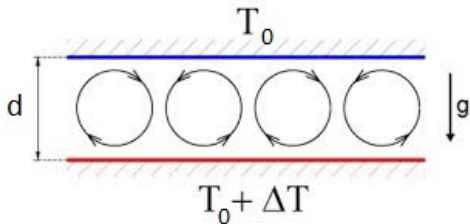
FDEPS Lecture 2, Kyoto, 28th November 2017

Section 2.

Convection in planetary interiors

2.1 Boussinesq Rayleigh-Bénard convection

Rayleigh-Bénard convection



Layer of liquid of depth d between two parallel horizontal plates heated from below.

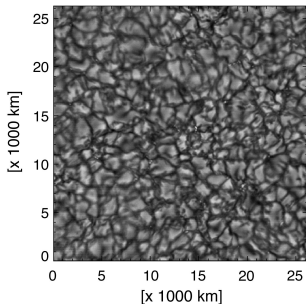
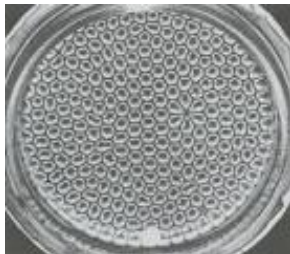
Hotter fluid expands, becomes less dense, and rises up. At the top, fluid cools, becomes denser and sinks back to the bottom.

This continual motion carries heat from the bottom of the layer to the top: heat transport by convection.

If the heating is small, the flow may be steady or vary slowly.

If the heating is strong, the flow is very turbulent.

Convection occurs on many different scales



Left image is Bénard's original experiment: layer depth about 1mm, convecting cells similar size. Fluid flow made visible by aluminium flakes which reflect the light.

Right image is a snapshot of the solar granulation. Each granule is hot fluid rising, and is typically 1000km across. This process transports the heat through the outer layers.

The Bénard cells are fairly steady, the solar granules are very turbulent.

Boussinesq approximation 1.

The density change that drives the convection is small, so we can ignore variations of density except when they are multiplied by gravity.

For a liquid, the density is

$$\rho = \rho_0(1 - \alpha T). \quad (2.1.1)$$

α is small, so mass conservation is

$$\nabla \cdot \mathbf{u} = 0. \quad (2.1.2)$$

Boussinesq equation of motion is

$$\frac{\partial \mathbf{u}}{\partial t} + (\mathbf{u} \cdot \nabla) \mathbf{u} = -\frac{1}{\rho_0} \nabla p - g(1 - \alpha T) \hat{\mathbf{z}} + \nu \nabla^2 \mathbf{u}. \quad (2.1.3)$$

which is the Navier-Stokes equation. Here p is the pressure, ν is the kinematic viscosity (units m^2s^{-1}).

Boussinesq approximation 2.

The temperature equation is

$$\frac{\partial T}{\partial t} + \mathbf{u} \cdot \nabla T = \kappa \nabla^2 T. \quad (2.1.4)$$

Here κ is the thermal diffusivity. It also has units m^2s^{-1} .

The thermal conductivity of the fluid is $K = \rho c_p \kappa$, where c_p is the specific heat at constant pressure.

This Boussinesq convection problem was discussed by Rayleigh in 1916. A nice treatment is given in Chandrasekhar, 1961.

The Boussinesq equations have a basic state conduction solution, where the fluid is at rest, and heat is transported only by thermal conduction.

As the temperature difference across the layer is increased, at a certain value the fluid starts to move.

The basic state solution has zero velocity and temperature fixed in time and a function of z only

$$0 = -\frac{1}{\rho_0} \nabla p - g(1 - \alpha T) \hat{z} \quad (2.1.5)$$

and

$$0 = \kappa \nabla^2 T. \quad (2.1.6)$$

The solution is

$$T = \bar{T} = T_0 + \Delta T(1 - z/d), \quad (2.1.7)$$

$$p = \bar{p} = p_0 - \rho_0 g z (1 - \alpha T_0 - \alpha \Delta T) - \frac{1}{2} \rho_0 g \alpha \Delta T z^2. \quad (2.1.8)$$

The heat flux carried by conduction is

$$F = -K \frac{dT}{dz} = \kappa \rho c_p \frac{\Delta T}{d} \text{ Watts per square metre.}$$

2.2 Linear theory of Rayleigh-Bénard convection

Stability of the basic state: onset of convection

We imagine the bottom plate temperature being slowly increased, i.e. ΔT slowly increased. There comes a point when the layer starts to convect.

Close to onset, the velocity will be small, so $\mathbf{u} \cdot \nabla \mathbf{u}$ will be small compared to $\nu \nabla^2 \mathbf{u}$, so we can neglect it. The temperature will only be slightly different from the basic state, so we write

$$T = T_0 + \Delta T(1 - z/d) + \theta \quad (2.2.1)$$

where θ is small compared to ΔT , and $p = \bar{p} + p'$.

The linearised dimensional equations are then

$$\frac{\partial \mathbf{u}}{\partial t} = -\frac{1}{\rho_0} \nabla p' + g\alpha\theta \hat{\mathbf{z}} + \nu \nabla^2 \mathbf{u}, \quad (2.2.2)$$

$$\nabla \cdot \mathbf{u} = 0, \quad (2.2.3)$$

$$\frac{\partial \theta}{\partial t} = u_z \Delta T/d + \kappa \nabla^2 \theta. \quad (2.2.4)$$

Non-dimensional equations 1.

Note that the two terms which can be neglected close to onset are $(\mathbf{u} \cdot \nabla)\mathbf{u}$ in the equation of motion, and $\mathbf{u} \cdot \nabla\theta$ in the temperature equation. They become important again as ΔT is increased.

We now write the equations in dimensionless form. The advantage of doing this is that the key dimensionless parameters appear, so we know how big the parameter space of our problem is.

Sometimes though it is useful to have dimensional equations as well, as then we can more easily see which terms are important in geophysical applications.

There are several possible choices, all lead to the same set of dimensionless parameters, but they appear in different places in the equations.

Non-dimensional equations 2.

Our choice is

$$\frac{\partial}{\partial t} = \frac{\kappa}{d^2} \frac{\partial}{\partial \tilde{t}}, \quad \nabla = \frac{1}{d} \tilde{\nabla}, \quad \mathbf{u} = \frac{\nu}{d} \tilde{\mathbf{u}}, \quad \theta = \frac{\nu \Delta T}{\kappa} \tilde{\theta}, \quad p' = \frac{\rho_0 \nu^2}{d^2} \tilde{p}' \quad (2.2.5)$$

giving

$$\frac{1}{Pr} \frac{\partial \tilde{\mathbf{u}}}{\partial \tilde{t}} = -\nabla \tilde{p}' + Ra \tilde{\theta} \hat{\mathbf{z}} + \tilde{\nabla}^2 \tilde{\mathbf{u}}, \quad \nabla \cdot \tilde{\mathbf{u}} = 0, \quad (2.2.6, 7)$$

$$\frac{\partial \tilde{\theta}}{\partial \tilde{t}} = \tilde{u}_z + \tilde{\nabla}^2 \tilde{\theta}. \quad (2.2.8)$$

Here

$$Ra = \frac{g \alpha \Delta T d^3}{\kappa \nu}, \quad Pr = \frac{\nu}{\kappa}, \quad (2.2.9)$$

are the two dimensionless parameters called the Rayleigh number and the Prandtl number.

Non-dimensional equations 3.

At this stage it is conventional to drop the tildes in the equations. This sometimes confuses students, because the untilded variables might be dimensionless or might have dimensions. But it is too tiresome to keep writing tildes, so you just have to be careful to check whether the variables are dimensionless or not. So the dimensionless linearised equations are

$$\frac{1}{Pr} \frac{\partial \mathbf{u}}{\partial t} = -\nabla p' + Ra\theta \hat{\mathbf{z}} + \nabla^2 \mathbf{u}, \quad (2.2.10)$$

$$\nabla \cdot \mathbf{u} = 0, \quad (2.2.11)$$

$$\frac{\partial \theta}{\partial t} = u_z + \nabla^2 \theta. \quad (2.2.121)$$

How big is the Rayleigh number?

The Rayleigh number is

$$Ra = \frac{g\alpha\Delta Td^3}{\kappa\nu}.$$

In a Bénard experiment with water, in S.I units (metres, seconds, kg, °K) $g \approx 10$, $\alpha \approx 10^{-4}$, $\Delta T \approx 1$, $d \approx 10^{-3}$, $\kappa \approx 10^{-5}$, $\nu \approx 10^{-4}$, for water.

$$Ra = \frac{10^{-12}}{10^{-9}} \approx 1000,$$

which as we will see is around the critical value for the onset of convection.

The Prandtl number ν/κ for water is usually taken as 6.8, for air it is about 0.7, and it is small for liquid metals.

For solar material, ΔT and d are very large, so the Rayleigh number is enormous, and it is very large in geophysical applications. So in practice Ra is massively supercritical. Is linear theory relevant in planets?

Boundary conditions

The temperature is fixed at $z = 0$ and the top boundary $z = 1$. So we need $\theta = 0$ at $z = 0$ and $z = 1$.

The fluid cannot penetrate the boundaries, so we must have $u_z = 0$ at $z = 0$ and $z = 1$.

The natural two remaining boundary conditions would be to set the horizontal velocities u_x and u_y zero at $z = 0$ and $z = 1$. From the continuity equation (8) this gives $du_z/dz = 0$ at $z = 0$ and $z = 1$.

However, Rayleigh noticed that if we take stress-free boundary conditions, $du_x/dz = du_y/dz = 0$, this gives $d^2u_z/dz^2 = 0$ on the boundaries and then there is a simple exact solution, so people often use stress-free boundary conditions (illustrative boundary conditions) to get an initial idea of the behaviour.

Solving the linear equations

We take the curl of the equation of motion (2.2.10). Recall that $\zeta = \nabla \times \mathbf{u}$ is the vorticity of the fluid, and

$$\zeta_z = \frac{\partial u_y}{\partial x} - \frac{\partial u_x}{\partial y}. \quad (2.2.13)$$

The curl of (2.2.10) gives the vorticity equation, and the z component gives

$$\frac{1}{Pr} \frac{\partial \zeta_z}{\partial t} = \nabla^2 \zeta_z. \quad (2.2.14)$$

The buoyancy force only generates horizontal vorticity, not vertical vorticity.

An important point is that $\nabla \times \nabla p = 0$, so taking the curl eliminates the awkward pressure term.

(2.2.13) is a diffusion equation, so if the vertical vorticity is zero at the boundaries, it diffuses away to zero everywhere, $\zeta_z = 0$.

The double curl equation

We take the curl of the vorticity equation, which is the double curl of the equation of motion (2.2.10).

$$\frac{1}{Pr} \nabla \times \nabla \times \frac{\partial \mathbf{u}}{\partial t} = Ra \nabla \times \nabla \times \theta \hat{\mathbf{z}} + \nabla \times \nabla \times \nabla^2 \mathbf{u} \quad (2.2.15)$$

Using $\nabla \cdot \mathbf{u} = 0$ and the vector identity $\text{curl curl} = \text{grad div} - \text{del}^2$, we get

$$\frac{1}{Pr} \frac{\partial}{\partial t} \nabla^2 u_z = Ra \nabla_H^2 \theta + \nabla^4 u_z, \quad \text{where} \quad \nabla_h^2 = \frac{\partial^2}{\partial x^2} + \frac{\partial^2}{\partial y^2}. \quad (2.2.16)$$

The double curl procedure looks complicated at first sight, but it is often the best way to solve the convection equations even if there are nonlinear equations and additional effects like rotation, magnetic fields or compressibility.

With the θ equation (2.2.11)

$$\frac{\partial \theta}{\partial t} = u_z + \nabla^2 \theta, \quad (2.2.17)$$

we now have just two scalar unknowns, u_z and θ .

We look for solutions which are periodic in x and y , and have time-dependence $\exp \sigma t$, $u_z = W(z) \exp[i(k_x x + k_y y) + \sigma t]$, $\theta = \Theta(z) \exp[i(k_x x + k_y y) + \sigma t]$ and putting these into (2.2.15) and (2.2.16), letting $a^2 = k_x^2 + k_y^2$,

$$\left(\frac{d^2}{dz^2} - a^2 - \frac{\sigma}{Pr} \right) \left(\frac{d^2}{dz^2} - a^2 - \sigma \right) \left(\frac{d^2}{dz^2} - a^2 \right) W + Ra a^2 W = 0. \quad (2.2.18)$$

This is a 6th order system of ODE's in z , so we need 6 boundary conditions.

Equation for the growth rate σ

With stress free boundary conditions, $W = 0$ and $D^2W = 0$, $D = d/dz$, and then $\Theta = 0$ is equivalent to $D^4u_z = 0$ since

$$\left(\frac{d^2}{dz^2} - a^2 - \frac{\sigma}{Pr}\right) \left(\frac{d^2}{dz^2} - a^2\right) W = Ra a^2 \Theta. \quad (2.2.19)$$

So the solution is $W(z) = \sin n\pi z$, for integer n , giving

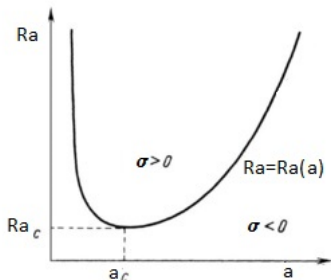
$$\sigma^2 + (n^2\pi^2 + a^2)\sigma(1 + Pr) + (n^2\pi^2 + a^2)^2 Pr - \frac{a^2 Ra Pr}{(n^2\pi^2 + a^2)} = 0. \quad (2.2.20)$$

This gives a steady solution $\sigma = 0$ when

$$Ra = Ra_c = \frac{(n^2\pi^2 + a^2)^3}{a^2}, \quad (2.2.21)$$

and if Ra is greater than this critical value, there is a solution with $\sigma > 0$ so the disturbance grows exponentially.

Dispersion relation for Ra



If $Ra < Ra_c$, σ has negative real part, so the disturbance decays away with time.

The values of a and n which minimise the critical Rayleigh number are the important critical values. $n = 1$ is always the minimum.

There is a minimum at $a_c = \pi/\sqrt{2}$, where $Ra_c = 27\pi^4/4 \approx 657$, Below this value all disturbances decay, while if $Ra > Ra_c$ a band of wavenumbers grow exponentially.

No-slip boundary case

In the more realistic no-slip case the boundary conditions are $W = DW = \Theta = 0$ on $z = 0, 1$, and then $\sin \pi z$ isn't a solution. However, the 6th order ODE can be integrated numerically with the no-slip boundary conditions, and the critical Rayleigh number plot looks similar.

In this case, $Ra_c \approx 1707.76$ and the minimising $a \approx 3.117$, close to π .

Lots of other cases are possible, e.g. one no-slip, one stress-free boundary, or fixed flux boundaries $d\Theta/dz = 0$.

Pattern selection in convection

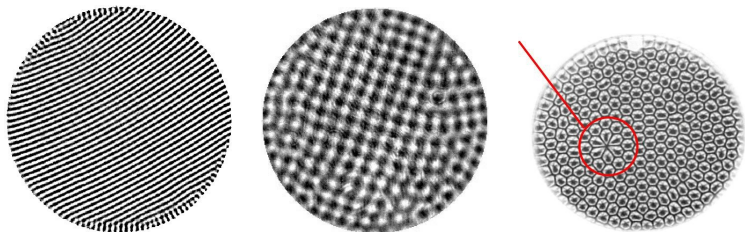
If Ra is just above Ra_c , a band of wavenumbers near $a = a_c = \sqrt{k_x^2 + k_y^2}$ can grow.

Initially there will be small random perturbations due to imperfections in the experiment, which will be made up of all wavenumbers. Only the unstable ones will grow, the others will decay, so the growing disturbance will contain only the unstable wavenumbers.

However, this does not give a unique pattern. There could be two-dimensional rolls aligned along the x axis, with $k_y = a_c$ and $k_x = 0$, or aligned along the y axis, with $k_x = a_c$ and $k_y = 0$.

Could also have square cells with $k_x = k_y = a_c/\sqrt{2}$. Even possible to have hexagonal cells.

Some observed convection patterns



Left: Two dimensional convection rolls. Middle: Square cells. Right: hexagonal cells.

Which mode actually occurs depends on the nonlinear terms. Although very small, over a very long time scale a preferred pattern generally appears.

Which pattern depends on the boundary conditions, and the Rayleigh and Prandtl numbers.

What happens if $\Delta T < 0$, so top boundary is hotter than lower boundary?

$Ra < 0$, and we have stably stratified fluid.

The limit $Ra \rightarrow -\infty$ corresponds to the small diffusion limit, and (2.2.20) becomes

$$\sigma^2 = \frac{a^2 Ra Pr}{n^2 \pi^2 + a^2}. \quad (2.2.22)$$

Restoring the dimensions,

$$\sigma^2 = -g \alpha \beta \frac{a^2 d^2}{n^2 \pi^2 + a^2 d^2}, \quad (2.2.23)$$

where $\beta = -\Delta T/d$, so β is now a positive temperature gradient.

Internal gravity waves

Taking the square root of this negative quantity,

$$\sigma = \pm i (g_{\alpha\beta})^{1/2} \frac{ad}{\sqrt{n^2\pi^2 + a^2d^2}}. \quad (2.2.24)$$

Since σ is now imaginary, the time dependence $\exp \sigma t$ corresponds to waves.

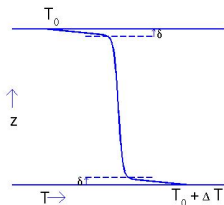
These waves are called internal gravity waves. The quantity

$$N = (g_{\alpha\beta})^{1/2}$$

is called the buoyancy frequency. If there is some viscous and thermal diffusion, then the internal gravity waves are damped. Physically, in a stably stratified layer, if a parcel of fluid moves upwards, it finds itself in less dense surroundings, so it falls back. The buoyancy is now a restoring force.

2.3 Nonlinear Rayleigh-Bénard convection

Nonlinear convection



As the Rayleigh number is increased, the horizontally averaged temperature profile changes.

Boundary layers appear, across which the temperature varies rapidly. The interior temperature becomes nearly constant.

The heat transport is mainly by conduction in the boundary layers, and by convection in the bulk interior.

If the boundary layer has thickness δ , the heat flux transported is

$$F = K \frac{\Delta T}{2\delta} \gg F_{basic} = K \frac{\Delta T}{d} \quad (2.3.1)$$

The dimensionless ratio $F/F_{basic} = Nu$, the Nusselt number.

Malkus-Howard convection theory

At large Rayleigh number, $Nu \approx d/2\delta$.

The Rayleigh number (2.2.9) is

$$Ra = \frac{g\alpha\Delta Td^3}{\kappa\nu}.$$

Malkus-Howard idea is that the thickness of the boundary layer makes it close to critical, so

$$Ra_{bl} = \frac{g\alpha\Delta T\delta^3}{\kappa\nu} \approx 10^3. \quad (2.3.2)$$

So

$$Ra = \frac{g\alpha\Delta Td^3}{\kappa\nu} \approx \frac{g\alpha\Delta T\delta^3}{\kappa\nu} 8Nu^3 \approx 8 \times 10^3 Nu^3, \quad (2.3.3)$$

giving

$$Nu \sim Ra^{1/3}. \quad (2.3.4)$$

Experiments suggest that the 1/3 law is close, though not all experiments agree.

Averaged heat flux

The temperature equation (2.1.4) is

$$\frac{\partial T}{\partial t} + \mathbf{u} \cdot \nabla T = \kappa \nabla^2 T.$$

Average over a horizontal plane at z ,

$$\langle a \rangle_h = \frac{1}{L_x L_y} \int_{-L_x/2}^{L_x/2} \int_{-L_y/2}^{L_y/2} a \, dx dy, \quad L_x \rightarrow \infty, L_y \rightarrow \infty. \quad (2.3.5)$$

$$\frac{\partial \langle T \rangle_h}{\partial t} + \langle \nabla \cdot (\mathbf{u} T) - T \nabla \cdot \mathbf{u} \rangle_h = \kappa \left\langle \frac{\partial^2 T}{\partial x^2} + \frac{\partial^2 T}{\partial y^2} + \frac{\partial^2 T}{\partial z^2} \right\rangle_h,$$

but averages of x or y derivatives are zero, and $\nabla \cdot \mathbf{u} = 0$. So

$$\frac{\partial \langle T \rangle_h}{\partial t} + \left\langle \frac{\partial}{\partial z} (u_z T) \right\rangle_h = \kappa \left\langle \frac{\partial^2 T}{\partial z^2} \right\rangle_h$$

Convective and conductive heat flux

We now take the time-average, so the $\partial/\partial t$ term goes,

$$\left\langle \frac{\partial}{\partial z} (u_z T) \right\rangle_h = \kappa \left\langle \frac{\partial^2 T}{\partial z^2} \right\rangle_h \quad (2.3.6)$$

true at every z level. Integrate from 0 to z' to get

$$\begin{aligned} \langle (u_z T) \rangle_{z'} &= \kappa \left\langle \frac{\partial T}{\partial z} \right\rangle_{z'} - \kappa \left\langle \frac{\partial T}{\partial z} \right\rangle_0 \\ \langle (u_z T) \rangle_{z'} - \kappa \left\langle \frac{\partial T}{\partial z} \right\rangle_{z'} &= F, \end{aligned} \quad (2.3.7)$$

because F is the heat flux conducted in at the bottom of the layer.

$\langle (u_z T) \rangle_{z'}$ is the convected heat flux at level z' and
 $-\kappa \langle \frac{\partial T}{\partial z} \rangle_{z'}$ is the conducted heat flux at level z' .

Note the convected heat flux is positive because hot fluid rises and cold fluid sinks.

Dissipation integral 1.

Equation of motion (2.1.3) is

$$\frac{\partial \mathbf{u}}{\partial t} + (\mathbf{u} \cdot \nabla) \mathbf{u} = -\frac{1}{\rho_0} \nabla p' + g\alpha T \hat{\mathbf{z}} + \nu \nabla^2 \mathbf{u},$$

taking out the hydrostatic part of the pressure. We take the scalar product of this with \mathbf{u} and average over x, y, z , and t

$$\mathbf{u} \cdot \frac{\partial \mathbf{u}}{\partial t} = \frac{\partial(\mathbf{u}^2/2)}{\partial t}, \quad \mathbf{u} \cdot (\mathbf{u} \cdot \nabla) \mathbf{u} = \nabla \cdot (\mathbf{u}(\mathbf{u}^2/2)), \quad \mathbf{u} \cdot \nabla p' = \nabla \cdot (p' \mathbf{u}),$$

and all these terms vanish when we average. For the last term

$$u_i \frac{\partial^2 u_i}{\partial x_j^2} = \frac{\partial}{\partial x_j} \left(u_i \frac{\partial u_i}{\partial x_j} \right) - \frac{\partial u_i}{\partial x_j} \frac{\partial u_i}{\partial x_j}, \quad (2.3.8)$$

giving

$$g\alpha \int_0^d \langle u_z T \rangle_{z'} dz' = \nu \int_0^d \left\langle \frac{\partial u_i}{\partial x_j} \frac{\partial u_i}{\partial x_j} \right\rangle_{z'} dz'. \quad (2.3.9)$$

Dissipation integral 2.

We now integrate the heat flux relation across the layer,

$$g\alpha \int_0^d \langle (u_z T) \rangle_{z'} - \kappa \left\langle \frac{\partial T}{\partial z} \right\rangle_{z'} dz' = g\alpha Fd \quad (2.3.10)$$

or

$$\nu \int_0^d \left\langle \left(\frac{\partial u_i}{\partial x_j} \right)^2 \right\rangle_{z'} dz' = g\alpha Fd - \kappa g\alpha \Delta T. \quad (2.3.11)$$

Now

$$Fd = Nu\kappa\Delta T, \quad g\alpha\Delta T = Ra\kappa\nu/d^3$$

So the dissipation integral can be written

$$\int_0^d \left\langle \left(\frac{\partial u_i}{\partial x_j} \right)^2 \right\rangle_{z'} dz' = \frac{\kappa^2 Ra(Nu - 1)}{d^3}. \quad (2.3.12)$$

Grossmann-Lohse theory 1.

This method is based on estimating where the majority of the dissipation comes from. It may be in the boundary layers, or it may be in the bulk.

In their picture there is a large scale flow with typical velocity U which develops a viscous boundary layer.

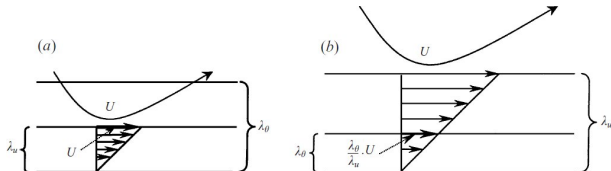


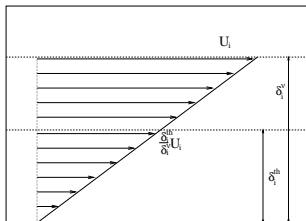
FIGURE 1. Sketch of the boundary layers, (a) for low Pr where $\lambda_u < \lambda_\theta$ and (b) for large Pr where $\lambda_u > \lambda_\theta$.

Depending on the Prandtl number, the viscous boundary layer will be inside or outside the thermal boundary layer. (2.3.12) gives

$$\nu \int_0^d \langle \nabla \mathbf{u} : \nabla \mathbf{u} \rangle dz = \frac{\nu^3}{d^3} RaNuPr^{-2}, \quad Nu \gg 1. \quad (2.3.13)$$

If the dissipation is mainly in the boundary layers, we analyse these boundary layers to estimate $\nu \langle \nabla \mathbf{u} : \nabla \mathbf{u} \rangle$. Different estimates also possible if dissipation is in the bulk.

$Pr > 1$ case, dissipation in boundary layers 1.



$Pr > 1$ means the thermal boundary layer is nested inside the viscous boundary layer.

U is large scale flow speed in bulk, δ^ν , δ^{th} viscous and thermal b.l. thicknesses.

Velocity at edge of thermal b.l. = $\delta^{th} U / \delta^\nu$.

Advection balances diffusion in the boundary layers, (2.1.3) is

$$\frac{\partial \mathbf{u}}{\partial t} + (\mathbf{u} \cdot \nabla) \mathbf{u} = -\frac{1}{\rho_0} \nabla p - g(1 - \alpha T) \hat{\mathbf{z}} + \nu \nabla^2 \mathbf{u}.$$

In the boundary layers dominant horizontal terms are $(\mathbf{u} \cdot \nabla) \mathbf{u}$ and $\nu d^2 \mathbf{u} / dz^2$.

This means that

$$\frac{U^2}{d} \sim \frac{\nu U}{(\delta^\nu)^2}. \quad (2.3.14)$$

Advection balances diffusion in the boundary layers in the temperature equation too, (2.1.4),

$$\frac{\partial T}{\partial t} + \mathbf{u} \cdot \nabla T = \kappa \nabla^2 T$$

In the boundary layers dominant terms here are $\mathbf{u} \cdot \nabla T$ and $\kappa d^2 T / dz^2$. This gives

$$\frac{UT}{d} \sim \frac{\kappa T}{(\delta^{th})^2}$$

giving

$$\frac{\delta^{th}}{\delta^\nu} \frac{UT}{d} \sim \frac{\kappa T}{(\delta^{th})^2}, \quad \frac{U^2}{d} \sim \frac{\nu U}{(\delta^\nu)^2}, \quad (2.3.15)$$

which gives

$$\delta^\nu / \delta^{th} = Pr^{1/3} \quad (2.3.16), \quad d / \delta^\nu = (Ud / \nu)^{1/2} = Re^{1/2}, \quad (2.3.17)$$

where Re is the Reynolds number of the flow.

$Pr > 1$ case, dissipation in boundary layers 3.

Since from (2.3.1) $F = K \frac{\Delta T}{2\delta^{th}}$, $F_{basic} = K \frac{\Delta T}{d}$,

$$Nu = F/F_{basic} \sim \frac{d}{2\delta^{th}} \sim \frac{d}{2\delta\nu} Pm^{1/3} \sim Re^{1/2} Pm^{1/3}. \quad (2.3.18)$$

Now we use the dissipation integral (2.3.13)

$$\int_0^d \langle \nabla \mathbf{u} : \nabla \mathbf{u} \rangle dz = \frac{\nu^2}{d^3} RaNuPr^{-2}, \quad Nu \gg 1.$$

Estimating the dissipation in the b.l.s,

$$\int_0^d \langle \nabla \mathbf{u} : \nabla \mathbf{u} \rangle dz \sim \frac{U^2}{\delta\nu} = \frac{Re^2 \nu^2}{d^2} \frac{Re^{1/2}}{d} = Re^{5/2} \frac{\nu^2}{d^3} \quad (2.3.19)$$

$$\Rightarrow RaNuPr^{-2} \sim Re^{5/2} \Rightarrow Nu \sim Ra^{1/4} Pr^{-1/12}. \quad (2.3.20)$$

2.4 Rotating flows

We now consider the onset of thermal convection in a rotating frame. Experimentally this is done by putting the convecting layer on a rotating turntable.

Also interested in convection in planets and stars, which usually rotate. Here the gravity is directed towards the centre of the planet or star, which rotates about its polar axis.

We can consider the rotational acceleration as providing a Coriolis force $2\rho\boldsymbol{\Omega} \times \mathbf{u}$, \mathbf{u} being the fluid velocity, and a centrifugal force $\rho\boldsymbol{\Omega} \times (\boldsymbol{\Omega} \times \mathbf{r})$. Centrifugal force can be written as a gradient of a potential, and so can be combined with the gravity force. Coriolis force is the crucial new ingredient.

The centrifugal terms

The effects of the Coriolis force are often more significant than the centrifugal force. If the rotation vector is in the z direction, and we take cylindrical polars (R, ϕ, z) then $\boldsymbol{\Omega} \times (\boldsymbol{\Omega} \times \mathbf{r}) = \Omega^2 R \hat{R}$. But this is just the gradient of the potential $\nabla \frac{1}{2} \Omega^2 R^2$.

We already have a term like this: gravity. So the centrifugal term just changes the gravity force. On Earth, the centrifugal term is quite small compared to the g , so its more convenient to think of the centrifugal force just changing gravity a bit rather than being a fundamentally new term.

In some experiments, the centrifugal term can be larger than gravity, which is a way of mimicking a radial gravity as found in a planet or star.

When are Coriolis terms important?

Compare $\mathbf{u} \cdot \nabla \mathbf{u}$ and $2\boldsymbol{\Omega} \times \mathbf{u}$. If the flow is varying on a length scale L , then $\mathbf{u} \cdot \nabla \mathbf{u} \sim U^2/L$ very roughly. $2\boldsymbol{\Omega} \times \mathbf{u} \sim \Omega U$ again roughly, so the ratio of these terms is the Rossby number

$$Ro = \frac{U}{\Omega L}. \quad (2.4.1)$$

If the Rossby number is large, Coriolis force won't be important but if it is small it will be an important part of the acceleration.

For the Earth $\Omega \sim 7 \times 10^{-5}$, a weather system can easily be 1000 km ($= 10^6$ m) across, and wind speeds are typically of order 10 m/s, giving $Ro \sim 1/7$ quite small, so rotation is important.

Same is true for ocean currents. Flows in rapidly rotating machinery can also have Ro small.

Taylor-Proudman theorem: geostrophic flow

Suppose we have slow, (low Ro), steady (no $\partial \mathbf{u} / \partial t$), inviscid flow. Then $2\rho \boldsymbol{\Omega} \times \mathbf{u} = -\nabla p + \rho \mathbf{g}$, including the centrifugal term in gravity.

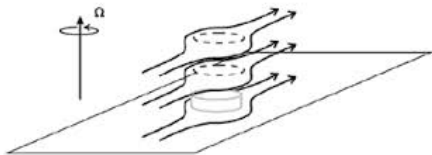
The curl of this equation gives

$$\begin{aligned} \nabla \times 2\rho(\boldsymbol{\Omega} \times \mathbf{u}) &= 2\rho \boldsymbol{\Omega}(\nabla \cdot \mathbf{u}) - 2\rho(\boldsymbol{\Omega} \cdot \nabla)\mathbf{u} = 0 \\ &\Rightarrow (\boldsymbol{\Omega} \cdot \nabla)\mathbf{u} = 0 \end{aligned} \quad (2.4.2)$$

since $\boldsymbol{\Omega}(\nabla \cdot \mathbf{u}) = 0$ if the fluid is incompressible. The velocity in a rotating fluid is independent of the rotation axis direction, z . The fluid has to flow in columns, independent of z .

This is the Taylor-Proudman theorem, and is the most important and remarkable result in rotating fluids. It is why rotating fluids behave so differently from non-rotating fluids.

Taylor's penny experiment



Taylor built an experiment in which he towed a penny along the bottom of a rotating tank of water. The column of water is made visible by adding dye.

All the water in the column of fluid above the penny moved along with the penny.

The fluid near the penny had to move with the penny as it was towed along, and by the z -independence of the flow, all the fluid in the column above has to move too.

The fluid is at rest and the tank is stirred by hand, then dye is added. Fluid disperses in three dimensions, very different from the 2D rotating case.

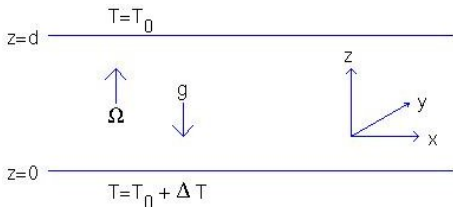
Dye in rotating fluid movie

The fluid is on a rotating turntable, and the camera is fixed in the frame of the turntable. The tank is stirred by hand, then dye is added. Main view is from above, but side view shown at the start. Fluid moves in two-dimensional sheets.

2.5 Plane layer rotating convection

Rotating Convection problems

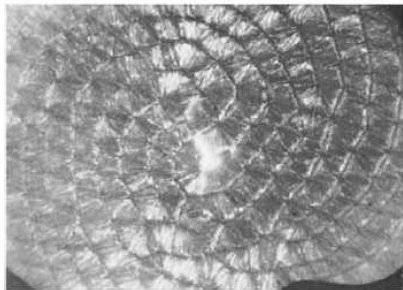
The rotating plane layer



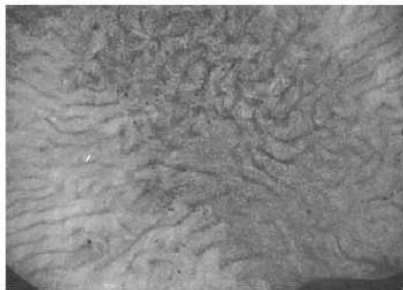
Rotation parallel to gravity, centrifugal acceleration negligible. This is the most common configuration for doing laboratory experiments, and the one where most is known about the nonlinear behaviour.

A standard Rayleigh-Bénard convection cell is put on a turntable rotating fast enough for the Rossby number to be small, but not so fast that centrifugal terms are important.

Plane layer experiments



(e)



(f)

FIGURE 4. Vertical view of thermal convection for different values of the Rayleigh and Taylor numbers. $P = 100$. The depth of the fluid is 0.7 cm and the field of view is about 15 cm. The axis of rotation is at the centre of the photographs in this and the following two figures.

Left: Bénard convection with no rotation. Right: Bénard convection with mild rotation. H.T.Rossby, JFM 36, 309 (1969). Note the smaller length scale cells in the rotating case.

Chandrasekhar, 1961. The linearised equation of motion is (2.2.2) with the Coriolis term,

$$\frac{\partial \mathbf{u}}{\partial t} + 2\Omega \hat{\mathbf{z}} \times \mathbf{u} = -\frac{1}{\rho} \nabla p' + g\alpha\theta \hat{\mathbf{z}} + \nu \nabla^2 \mathbf{u}. \quad (2.5.1)$$

The temperature equation is

$$\frac{\partial \theta}{\partial t} = \beta u_z + \kappa \nabla^2 \theta, \quad (2.5.2)$$

$\beta = \Delta T/d$, and the Boussinesq continuity equation is

$$\nabla \cdot \mathbf{u} = 0, \quad (2.5.3)$$

since the fluid is incompressible. Rayleigh-Bénard + Coriolis term.

Vorticity equation

Take the curl to eliminate pressure, forming the vorticity equation.
Recall

$$\nabla \times (\mathbf{a} \times \mathbf{b}) = (\mathbf{b} \cdot \nabla)\mathbf{a} - (\mathbf{a} \cdot \nabla)\mathbf{b} + \mathbf{a}\nabla \cdot \mathbf{b} - \mathbf{b}\nabla \cdot \mathbf{a},$$

so $\nabla \times (\hat{\mathbf{z}} \times \mathbf{u}) = -\partial\mathbf{u}/\partial z$.

So

$$\frac{\partial \zeta}{\partial t} - 2\Omega \frac{\partial \mathbf{u}}{\partial z} = g\alpha \nabla \times \theta \hat{\mathbf{z}} + \nu \nabla^2 \zeta. \quad (2.5.4)$$

Note that z-vorticity can be created by fluid stretching in the z-direction. Vertical vorticity is now coupled into the linear system in the rotating case.

Inertial waves 1.

We first retain the $\partial/\partial t$ term but ignore the others (assume temporarily the fluid is homogeneous and inviscid) to get

$$\frac{\partial \zeta}{\partial t} - 2\Omega \frac{\partial \mathbf{u}}{\partial z} = 0. \quad (2.5.5)$$

The curl of this gives

$$\frac{\partial}{\partial t} \nabla^2 \mathbf{u} + 2\Omega \frac{\partial \zeta}{\partial z} = 0 \quad (2.5.6)$$

and eliminating ζ gives the wave equation

$$\frac{\partial^2}{\partial t^2} \nabla^2 \mathbf{u} = -4\Omega^2 \frac{\partial^2 \mathbf{u}}{\partial z^2}. \quad (2.5.7)$$

These are inertial waves. Vortex lines behave like stretched strings: if you bend them they vibrate about the straight position.

Inertial waves 2.

The solution is

$$\mathbf{u} = \mathbf{u}_0 \exp i(k_x x + k_y y + k_z z - \omega t), \quad (2.5.8)$$

and then

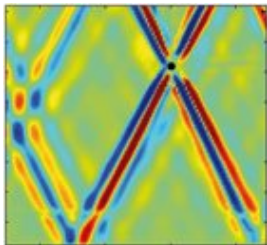
$$\omega^2 = \frac{4\Omega^2 k_z^2}{k^2}, \quad k^2 = k_x^2 + k_y^2 + k_z^2, \quad (2.5.9)$$

is the inertial wave dispersion relation. Note that columnar motion has k_z small, so ω is small. Also we must have $|\omega| < 2\Omega$.

If viscosity is restored, waves are damped.

Note that if we let $\omega/2\Omega = \cos \theta$, $k_z/|\mathbf{k}| = \cos \theta$, so waves of given frequency travel with a definite angle θ to the z axis.

Inertial waves in the laboratory



Inertial waves excited by a vibrating cylinder in a rotating water tank. If $\boldsymbol{\Omega} \cdot \mathbf{k} = |\boldsymbol{\Omega}| |\mathbf{k}| \cos \theta$, $\cos \theta$ is uniquely set by ω , so waves travel at specific angle.

These waves have not been seen in the Earth's core, because we have no means of detecting them, but they are seen in rotating MHD experiments.

If $\boldsymbol{\Omega}$ nearly perpendicular to \mathbf{k} , the waves are much slower. If $\mathbf{k} \cdot \boldsymbol{\Omega} = 0$, no z -dependence, the motion is called geostrophic. If $k_z \ll k_{\perp}$ it is called quasi-geostrophic (QG). QG waves are called Rossby waves.

The z-component of the vorticity equation is

$$\frac{\partial \zeta_z}{\partial t} - 2\Omega \frac{\partial u_z}{\partial z} = \nu \nabla^2 \zeta_z, \quad (2.5.10)$$

and the z-component of the double curl gives

$$\frac{\partial}{\partial t} \nabla^2 u_z + 2\Omega \frac{\partial \zeta_z}{\partial z} = g\alpha \nabla_H^2 \theta + \nu \nabla^4 u_z, \quad (2.5.11)$$

and then (2.5.2), (2.5.10) and (2.5.11) give

$$\begin{aligned} \left(\frac{\partial}{\partial t} - \nu \nabla^2\right)^2 \left(\frac{\partial}{\partial t} - \kappa \nabla^2\right) \nabla^2 u_z + 4\Omega^2 \left(\frac{\partial}{\partial t} - \kappa \nabla^2\right) \frac{\partial^2 u_z}{\partial z^2} \\ = g\alpha\beta \nabla_H^2 \left(\frac{\partial}{\partial t} - \nu \nabla^2\right) u_z. \end{aligned} \quad (2.5.12)$$

where $\nabla_H^2 = \partial^2/\partial x^2 + \partial^2/\partial y^2$.

For stress-free, constant temperature boundaries, the solution is

$$u_z = A \sin \pi z \exp i(k_x x + k_y y) \exp \sigma t, \quad (2.5.13)$$

which satisfies all the stress-free boundary conditions, and we get

$$\begin{aligned} (\sigma + \pi^2 + a^2)^2 (Pr\sigma + \pi^2 + a^2)(\pi^2 + a^2) + (Pr\sigma + \pi^2 + a^2)E^{-2}4\pi^2 \\ = a^2 Ra(\sigma + \pi^2 + a^2) \end{aligned} \quad (2.5.14)$$

where

$$E = \frac{\nu}{\Omega d^2}, \quad Ra = \frac{g\alpha\beta}{\kappa\nu}, \quad a^2 = k_x^2 + k_y^2, \quad Pr = \frac{\nu}{\kappa}, \quad (2.5.15)$$

and E is the Ekman number, Ra the Rayleigh number, and Pr the Prandtl number.

Steady modes 1.

First look for neutral modes for the onset of steady convection, $\sigma = 0$. Then (2.5.14) simplifies to

$$Ra_{steady} = \frac{(\pi^2 + a^2)^3}{a^2} + \frac{4\pi^2}{E^2 a^2}. \quad (2.5.16)$$

Note that as $E \rightarrow \infty$ we get the classic Rayleigh-Bénard dispersion relation. If E is finite, the onset of convection is delayed by rotation, so rotation is normally a **stabilising** influence.

Letting $x = a^2/\pi^2$,

$$\frac{dRa_{steady}}{dx} = 0 \quad \text{when} \quad 2x^3 + 3x^2 = 1 + \frac{4E^{-2}}{\pi^4}. \quad (2.5.17)$$

As $E \rightarrow 0$, $x^3 \sim 2E^{-2}/\pi^4$ or

$$a \sim (2\pi^2)^{1/6} E^{-1/3}, \quad (2.5.18)$$

So a is large for rapid rotation which means onset occurs as tall thin columns, width $\sim E^{1/3}$.

This is because viscosity is essential for convection, and at small E viscosity can only act over short length scales. So the columns have to be tall and thin. Note this columnar structure is the best the fluid can do to obey the Taylor-Proudman theorem.

In the small E limit,

$$Ra \sim 3a^4 \sim 3(2\pi^2)^{2/3} E^{-4/3} \quad (2.5.19)$$

so the critical Rayleigh number gets very large at small E .

Oscillatory modes 1.

To see if we can get oscillatory modes we let $\sigma = i\omega$ in (2.5.14) and look at real and imaginary parts. This gives

$$-\omega^2 Pr(\pi^2 + a^2) + (\pi^2 + a^2)^3(2 + Pr) + 4PrE^{-2}\pi^2 = a^2 Ra, \quad (2.5.20)$$

$$-\omega^2(1 + 2Pr)(\pi^2 + a^2) + (\pi^2 + a^2)^3 + 4E^{-2}\pi^2 = a^2 Ra. \quad (2.5.21)$$

Could eliminate ω^2 between these to get the critical Ra for oscillatory modes, Ra_{osc} . However, first note that (2.5.20) - $Pr \times$ (2.5.21) gives

$$2\omega^2 Pr^2(\pi^2 + a^2) + 2(\pi^2 + a^2)^3 = a^2 Ra(1 - Pr), \quad (2.5.22)$$

which shows that oscillatory modes can only occur if $Pr < 1$.

Oscillatory modes 2.

However, if $Pr < 1$ it is possible to find oscillatory modes.

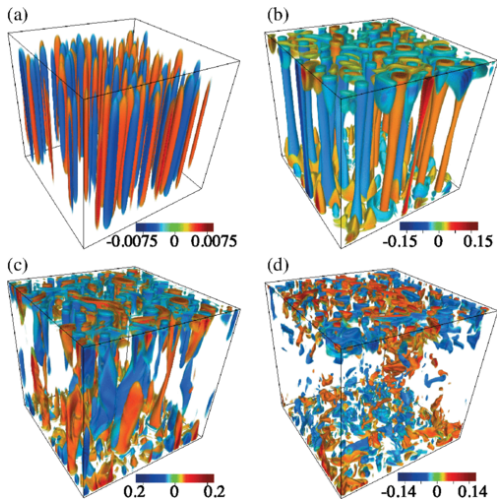
Indeed, if Pr is sufficiently small the minimum critical Rayleigh number for oscillatory convection is lower than the minimum critical for steady convection, so if the Rayleigh number is slowly increased, oscillatory modes onset first at low Prandtl number.

In the limit $E \rightarrow 0$ the critical value of Pr for oscillatory modes to onset first is $Pr = 0.6766$.

As with non-rotating case, other boundary conditions, e.g. no-slip boundaries can be dealt with numerically. Nothing radically different happens.

2.6 Nonlinear rotating convection

Plane layer model: nonlinear simulations

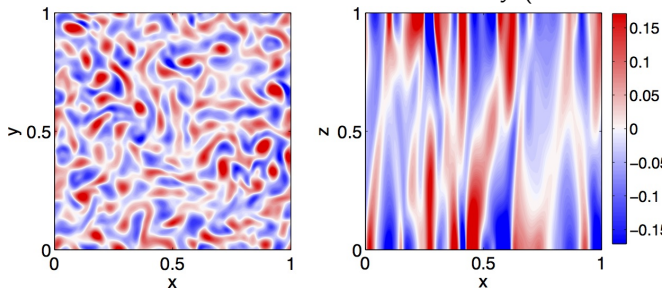


Numerical simulations (Stellmach et al. 2014) at $E = 10^{-7}$. These are for no-slip boundaries, and the temperature perturbation is shown. (a) just above critical Ra , (b-d) at increasing Ra . $Pr = 7$. In (a) the local Rossby number $Ro = U/\ell\Omega$ is small, but inertia becomes important at higher Ra .

Near the onset of convection

For Ra just above Ra_c :

Horizontal and vertical slices of the axial vorticity ($E = 5 \times 10^{-6}$):



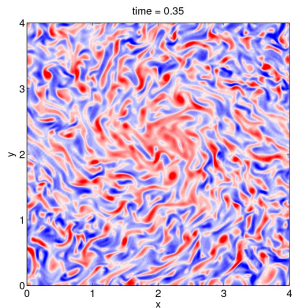
Convective structures near the onset:

- Multitude of small vortices of either sign, driven directly by buoyancy
- Elongated structures with horizontal size decreasing with Ekman number
- Mid-plane antisymmetry of the axial vorticity

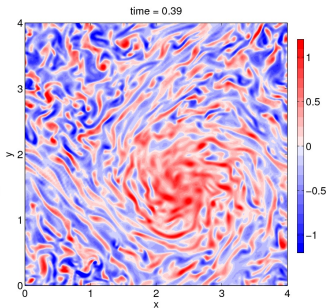
Formation of large-scale vortices (LSV)

For $Ra \approx 3Ra_c$:

During the growing phase:



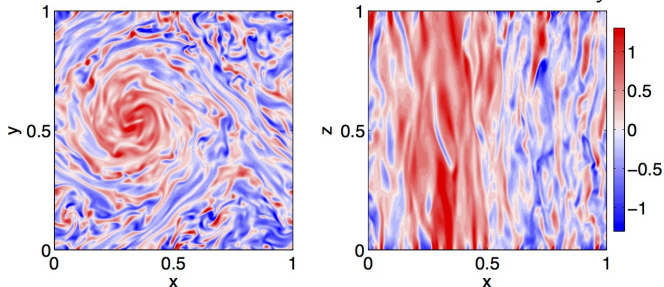
During the saturated phase:



Clustering of small cyclonic vortices into a fast cyclonic circulation.
Convective vortices advected by a slower anticyclonic circulation.
Regions of intense shear: horizontal stretching of the convective vortices.

Structure of the large-scale vortices (LSV)

Horizontal and vertical slices of the axial vorticity



Flow dominated by a cyclone: never an anticyclone. Always grows to the box size.

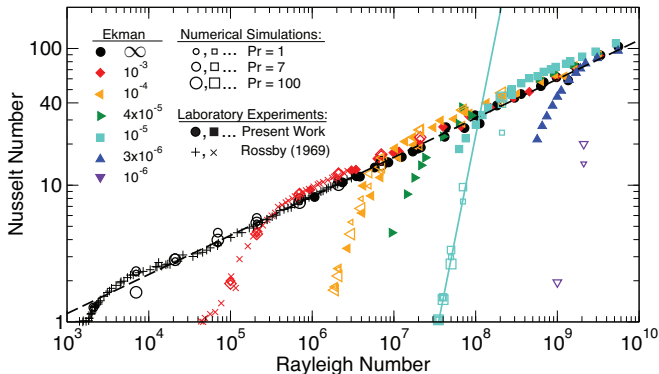
LSVs are mostly z -invariant, but outside the LSV small structures are z -dependent.

Periodic horizontal boundary conditions: horizontal average of ζ_z is zero.

LSVs essentially horizontal motions (not a convective structure)

Nusselt number versus Rayleigh number

King et al. 2012.



Rotation delays the onset of convection, but the Nusselt number then grows rapidly.

When $Ro \sim O(1)$ the Nusselt number curve goes back to the nonrotating value. LSVs only found on the rapidly rotating part of the curve.

2.7 Rotating spherical connection: Busse annulus

Rotating convection in spheres

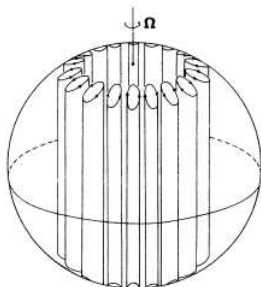
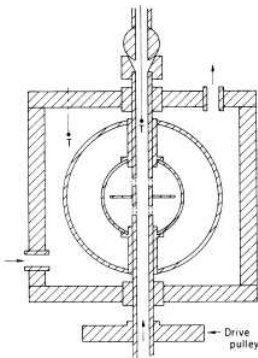
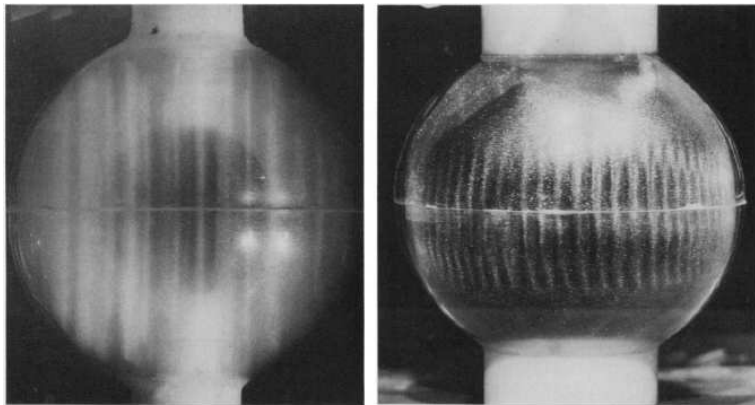


Fig. 1 (left). Qualitative sketch of convective motions in a rotating, self-gravitating fluid sphere. Fig. 2 (right). Schematic diagram of experimental apparatus; T denotes thermocouple.



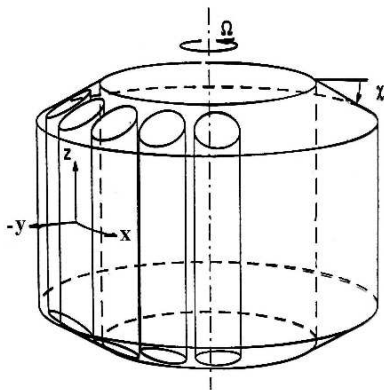
Left. Sketch of the nature of convection between concentric rotating spheres. Right. Experimental apparatus. Centrifugal acceleration much larger than gravity. Inner sphere cooled. F.H. Busse and C.R. Carrigan, *Science*, 191, 81-83 (1976).

Rotating convection experiment in a sphere



Snapshots of their convection experiments in rapidly rotating spheres. Left: small inner sphere. Right: large inner sphere. Note the convection columns.

The Busse annulus model



Busse annulus captures the essential feature, the sloping boundaries. We assume the flow is almost 2D, so the horizontal motion is described by a streamfunction ψ , but there is a small slope χ to the boundaries. Gravity radially inward, temperature $T = T_0$ at $y = 0$, $T = T_0 + \Delta T$ at $y = d$, so $T = T_0 + (y/d)\Delta T + \theta$.

Gap-width is d , annulus height is L .

We let $u_x = -\partial\psi/\partial y$ and $u_y = \partial\psi/\partial x$. The temperature gradient driving the convection is in the y direction.

The temperature gradient can now drive z -vorticity, and the z -component of the linearised vorticity equation is now

$$\frac{\partial \zeta_z}{\partial t} - 2\Omega \frac{\partial u_z}{\partial z} = -g\alpha \frac{\partial \theta}{\partial x} + \nu \nabla^2 \zeta_z, \quad (2.7.1)$$

since gravity is in the y -direction, perpendicular to the rotation vector. So buoyancy drives z -vorticity directly.

Average over z , column length H ,

$$\begin{aligned} \frac{\partial}{\partial t} \frac{1}{H} \int_0^H \zeta_z dz - \frac{2\Omega}{H} [u_z(H/2) - u_z(-H/2)] &= -\frac{g\alpha}{H} \frac{\partial}{\partial x} \int_0^H \theta dz \\ &+ \frac{\nu}{H} \nabla^2 \int_0^H \zeta_z dz \end{aligned} \quad (2.7.2)$$

Now since the slope at the boundaries is a small angle χ , $u_z = \pm\chi u_y$ on the endwalls $z = \pm H/2$, and we replace the vorticity and temperature with its z average,

$$\frac{\partial \zeta_z}{\partial t} - \frac{4\Omega\chi}{H} u_y = -g\alpha \frac{\partial \theta}{\partial x} + \nu \nabla^2 \zeta_z. \quad (2.7.3)$$

Since we have averaged out the z -dependence, and the z -component of velocity is small compared to the x and y components, we can introduce a streamfunction

$$\mathbf{u} = -\nabla \times \psi \hat{\mathbf{z}} \quad (2.7.4)$$

so then $\zeta_z = \nabla_H^2 \psi$, $u_y = \partial \psi / \partial x$.

So we get after non-dimensionalising the linearised equations

$$\frac{\partial \zeta_z}{\partial t} - \beta \frac{\partial \psi}{\partial x} = -Ra \frac{\partial \theta}{\partial x} + \nabla^2 \zeta_z, \quad (2.7.5)$$

$$Pr \frac{\partial \theta}{\partial t} = -\frac{\partial \psi}{\partial x} + \nabla^2 \theta, \quad (2.7.6)$$

$$\zeta_z = \nabla_H^2 \psi, \quad (2.7.7)$$

where

$$Ra = \frac{g\alpha\Delta T d^3}{\kappa\nu}, \quad \beta = \frac{4\Omega\chi d^3}{\nu H}. \quad (2.7.8)$$

Note that in the annulus model β is no longer the temperature gradient! β plays the role of the inverse Ekman number here. It is also related to the beta-effect in geophysical fluid dynamics.

Busse annulus dispersion relation 1.

We look for solutions

$$\psi = A \sin \pi y \exp i(kx - \omega t) \quad (2.7.9)$$

Substituting in to (2.7.5)-(2.7.7) gives

$$\begin{aligned} & -i\omega(\pi^2 + k^2)(\pi^2 + k^2 - i\omega Pr) + ik\beta(\pi^2 + k^2 - i\omega Pr) \\ & = k^2 Ra - (\pi^2 + k^2)^2(\pi^2 + k^2 - i\omega Pr). \end{aligned} \quad (2.7.10)$$

The imaginary part of this gives

$$\omega = \frac{\beta k}{(\pi^2 + k^2)(1 + Pr)} \quad (2.7.11)$$

and the real part gives

$$Ra = \frac{(\pi^2 + k^2)^3}{k^2} + \frac{\beta^2 k^2 Pr^2}{(\pi^2 + k^2)(1 + Pr)^2}. \quad (2.7.12)$$

Busse annulus dispersion relation 2.

In the annulus model convection is always oscillatory. Waves described by (2.7.11) are thermal Rossby waves.

If we drop the buoyancy term and the viscosity, (2.7.5) and (2.7.7) give (2.7.11) with $Pr = 0$ which is the standard Rossby wave dispersion relation. The restoring force comes from the sloping boundaries. If a column of fluid moves towards the axis, it stretches and the vortex tension brings it back.

Since $\omega/k > 0$ these Rossby waves travel eastward. In geophysical fluid dynamics, the beta effect comes from a variation in the Coriolis parameter at different latitudes, and has the opposite sign, so in the atmosphere Rossby waves travel westward.

If we take the large β limit (low viscosity), and minimise Ra over k , the optimising k is large, so we have tall thin columns again. In fact the lowest critical Ra occurs when

$$k = \frac{\beta^{1/3} Pr^{1/3}}{2^{1/6}(1 + Pr)^{1/3}}, \quad \omega = \frac{\beta^{2/3} 2^{1/6}}{Pr^{1/3}(1 + Pr)^{2/3}},$$
$$Ra = \frac{3\beta^{4/3} Pr^{4/3}}{2^{2/3}(1 + Pr)^{4/3}}. \quad (2.7.13)$$

Note that the dependencies are very similar to those in plane layer convection with β playing the role of E^{-1} .

If we add in the advection terms for ζ_z and θ we get the nonlinear Busse annulus equations

$$\frac{\partial \zeta_z}{\partial t} + (\mathbf{u} \cdot \nabla) \zeta_z - \beta \frac{\partial \psi}{\partial x} = -Ra \frac{\partial \theta}{\partial x} + \nabla^2 \zeta_z, \quad (2.7.14)$$

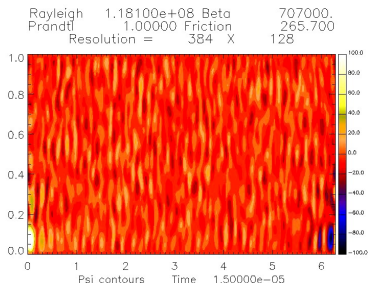
$$Pr \left(\frac{\partial \theta}{\partial t} + (\mathbf{u} \cdot \nabla) \theta \right) = -\frac{\partial \psi}{\partial x} + \nabla^2 \theta, \quad (2.7.15)$$

$$\zeta_z = \nabla_H^2 \psi. \quad (2.7.16)$$

These can be integrated in time fairly easily, because they are only two-dimensional in x and y .

It is also possible to add in a term proportional to $-\zeta_z$ in (2.7.14) (Rotvig and Jones, 2006) to represent friction acting on the top and bottom boundaries.

Zonal jet formation in the annulus



The x direction is eastward, and the y direction is towards the rotation axis.

These simulations have

$$\beta = 7 \times 10^5 \text{ and } Ra = 2.5 Ra_{crit}.$$

Multiple jet solutions occur when there is some bottom friction, stress-free boundaries give fewer jets.

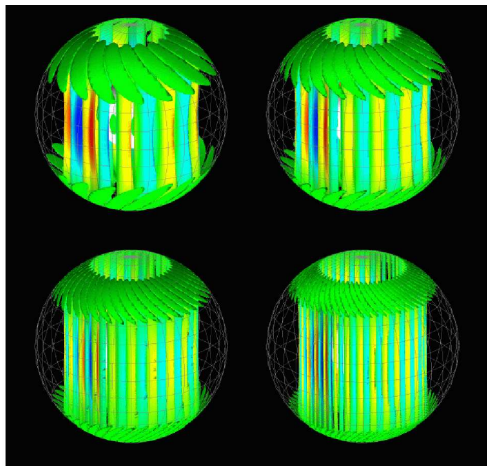
The Busse annulus model assumes the angle of the boundary χ is small. The vertical velocity is then small, and the 2D equations are asymptotically valid as $\chi \rightarrow 0$.

In spherical geometry, the angle χ is not small, but nevertheless flow behaves similarly to that in full spherical simulations.

In the QGA, the 2D annulus equations in s and ϕ are integrated forward in time, but the varying slope of the boundary is taken into account.

The QGA model is popular, because 2D simulations are much less demanding than 3D simulations.

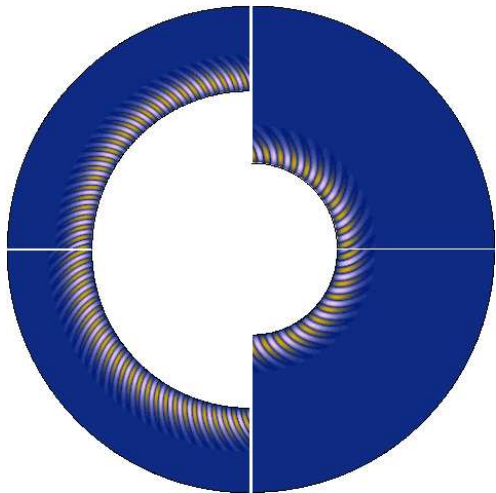
Onset of convection in a sphere



Contours of axial vorticity.
Sequence with
 $E = 3 \times 10^{-5}$,
 10^{-5} , $E = 3 \times 10^{-6}$, 10^{-6} .
Picture by Emmanuel
Dormy.

Note convection onsets
first near tangent cylinder
(where field is strongest in
the dynamo). Convection
columns get thinner at
smaller E .

Rapidly rotating convection: equatorial sections



Contours of axial vorticity at $E = 10^{-7}$. Top, numerical calculations. Bottom asymptotic theory. Left internal heating, right differential heating.

For radius ratio 0.35, internal heating sets in first in the interior. Note good agreement between asymptotics and numerics. Note also spiralling nature of solution.

2.8 Scaling laws in convection

No simulations can reach the very small Ekman number found in planetary cores.

The aim of scaling law work is to understand how key quantities such as the convective velocity and heat flux scale with Ekman number. The hope is that we can then use simulations at relatively large E to estimate what will happens at small E .

Physical arguments are based on the force balance:

Inertia Coriolis Buoyancy Lorentz Viscous

Heat transport and typical velocity

In nonlinear theories, the temperature fluctuation has to be estimated from heat flux,

$$F_{conv} = \int_S \rho c_p U_r \theta dS / 4\pi r^2 \sim \rho c_p U_* T_*, \quad (2.8.1)$$

where U_* and T_* are root mean square velocity and temperature fluctuations, and c_p is the specific heat.

This assumes that there is a strong correlation between hot fluid and rising fluid. In rotating convection this is not so clear!

In strongly nonlinear convection, balance is between inertia and buoyancy, the mixing length theory, so

$$U_*^2/d \sim g\alpha T_* \sim g\alpha F / \rho c_p U_*. \quad (2.8.2)$$

In compressible convection d is usually taken as the density scale height, in Boussinesq convection as the distance between the boundaries.

Mixing length theory: $U_*^2/d \sim g\alpha T_* \sim g\alpha F/\rho c_p U_*$.

Gives the Deardorff velocity

$$U_* \sim \left(\frac{g\alpha Fd}{\rho c_p} \right)^{1/3} \quad (2.8.3)$$

which works well in laboratory experiments.

In the core, for 1TW of convective heat flux this gives U_* about 10 times too big. Suggests that rotation/magnetic field is slowing down the convection.

Vorticity equation

$$\mathbf{u} \cdot \nabla \zeta - 2(\boldsymbol{\Omega} \cdot \nabla) \mathbf{u} = \nabla \times g\alpha\theta \hat{\mathbf{r}}, \quad (2.8.4)$$

ignoring viscosity. This gives

$$\frac{U_*^2}{L_\perp^2} \sim \frac{\Omega U_*}{d} \sim \frac{g\alpha\theta}{L_\perp}. \quad (2.8.5)$$

Here U_* is typical convective velocity. $|\omega| \sim U_*/L_\perp$,

$d = r_{cmb} - r_{icb}$,

L_\perp is length scale perpendicular to z , the roll axis.

$$L_\perp \sim \left(\frac{U_* d}{\Omega} \right)^{1/2} \sim \left(\frac{5 \times 10^{-4} \times 2 \times 10^6}{7 \times 10^{-5}} \right)^{1/2} \sim 4 \text{ km} \quad (2.8.6)$$

L_\perp is Rhines length, balance of inertia and Coriolis. On longer length scales, inertia \ll Coriolis.

Convective heat flux per square metre $F_{conv} \sim \rho c_p U_* \theta$.

Eliminate θ to get

$$\frac{U_*}{\Omega d} = Ro \sim \left(\frac{g \alpha F_{conv}}{\rho c_p \Omega^3 d^2} \right)^{2/5} = (Ra_Q)^{2/5}. \quad (2.8.7)$$

For compositional convection, $g \alpha F_{conv}$ is replaced by the buoyancy flux.

Fitting data from dynamo simulations, CA2006 obtained

$$Ro = 0.85 Ra_Q^{0.41} \quad (2.8.8)$$

very close to inertial scaling. Predicted velocity can be compared with westward drift velocity in the Earth's core.